Unoccupied surface states on Ta(100) observed with inverse photoemission

R. A. Bartynski* and T. Gustafsson
Department of Physics, University of Pennsylvania, Philadelphia, Pennsylvania 19104-6396
and Laboratory for Research on the Structure of Matter, University of Pennsylvania, Philadelphia, Pennsylvania 19104-3859
(Received 7 July 1986)

In an attempt to understand the interrelation of surface electronic structure and surface geometry, we have used inverse photoemission to measure the unoccupied surface states on the (100) face of tantalum. Tantalum has one fewer electron than tungsten and the Ta(100) surface is bulk terminated at room temperature, while the W(100) surface is reconstructed. We observe several well-defined features within 2 eV of the Fermi level in the Ta(100) spectra that show strong sensitivity to surface contamination and are therefore associated with surface states and/or resonances. It is difficult to relate the observed features to the W surface states in an empirical way. The two-dimensional dispersion of these states is rather flat, as expected for d-derived states. The results are compared in detail to a recent slab calculation. The spectral intensity of the surface states is significantly weaker than for states on Cu and Ag, a fact that we relate to the higher density of unoccupied states immediately above the Fermi level for the $5d$ metals as compared to the $3d$ metals. A peak seen near the Fermi level for the normal-incidence spectrum is related to a strong surface state or resonance below the Fermi level broadened so that it spans the Fermi level. The most likely origin of this broadening is coupling to bulk bands.

I. INTRODUCTION

It has been known for several years that the (100) surfaces of W and Mo undergo a reversible temperature-dependent reconstruction.[1-3] The superstructure observed on W(100) at low temperatures is referred to as a $(\sqrt{2}\times\sqrt{2})R45°$ structure. At room temperature and above, a (1×1) structure is observed. It is commonly believed that, in the reconstructed phase, the surface atoms are displaced in rows along the $\langle 011\rangle$ direction, adjacent rows being displaced in opposite directions.[2,3] Considerable uncertainty still exists about the exact atomic positions in the reconstructed phase, as well as to the nature of the (1×1) phase. Figure 1 shows the geometry of the bcc (100) surface in real space. The open circles represent the ideal (1×1) surface. The shaded circles show the proposed[2,3] displacements, which result in the observed reconstruction. The surface Brillouin zones (SBZ's) appropriate for these two structures are shown in the lower half of the figure.

W(100) has a large number of well documented[4-9] surface states close to the Fermi level, which have been linked to the occurrence of the phase transition. While early theories[6,8] suggested the reconstruction was caused directly by a surface charge density wave, it was eventually demonstrated that these effects are too small to induce structural changes.[7] Instead, it was proposed that the W(100) surface is inherently unstable to several types of reconstructions and that the surface states merely determine which of these reconstructions is favored.[7] Angle-resolved photoemission measurements[4] of these states demonstrated that their detailed dispersions were incompatible with their playing a major role in driving the reconstruction.

Tantalum is one column to the left of tungsten in the

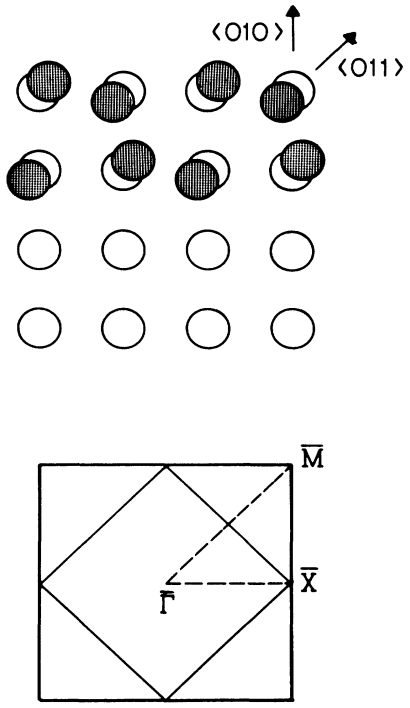

FIG. 1. The real- and reciprocal-space geometry of the bcc (100) surface. The open circles represent the unreconstructed surface. The shaded circles show the atomic displacements proposed to account for the $(\sqrt{2}\times\sqrt{2})R45°$ symmetry observed with LEED on W(100). The reconstructed (light lines) and unreconstructed (bold lines) surface Brillouin zones are shown in the lower half of the figure.

Periodic Table and also crystallizes in the bcc structure. The band structure of Ta throughout the Brillouin zone (BZ) corresponds closely to that of W with the Fermi level lowered by about 1.8 eV (Ref. 10). The Fermi level of Ta goes through the middle of the d band, and a large manifold of unoccupied d states will therefore exist. Ta(100) does not reconstruct over the temperature range of 15—650 K (Refs. 11 and 12). Based on a 5-layer slab calculation for Ta(100), Krakauer has proposed that this is because certain surface states, which are occupied on W(100), are *un*occupied on Ta(100) and therefore cannot play a role in the reconstruction.[10]

Motivated by these considerations, we have used inverse photoemission in an effort to identify unoccupied surface states on Ta(100). Boiziau *et al.*[13] have reported angle integrated spectra obtained from polycrystalline samples at $\hbar\omega = 9.7$ eV. Their spectra, corrected for an inelastic background originating from electron-hole pair creation, show good agreement with the predicted density of states (DOS) (Ref. 14) above the Fermi level. Our angle-resolved measurements obtained from a single-crystal sample show several spectral features which correspond to unoccupied d-like surface states. A large number of free-electron-like unoccupied surface states have been observed[15,16] with inverse photoemission on other metal surfaces, but our results apparently constitute the first experimental observation of unoccupied d-like surface states. These states differ from sp-derived surface states seen above the Fermi level on other surfaces mainly in that their dispersions do not follow free-electron-like parabolas. Good qualitative agreement between the measured dispersions and those predicted by Krakauer's calculation[10] is obtained. There are quantitative differences, however, in that the experimentally observed surface states or surface resonances exist in different regions of the SBZ than expected from the calculation. It is difficult to judge whether these disagreements are significant since they are on the order of the numerical uncertainty of the calculation. Very recently, the occupied surface states of Ta(100) have been the subject of a comprehensive study using angle-resolved photoemission,[17] and, where possible, we will discuss our data in relation to those results.

II. EXPERIMENTAL

The experimental apparatus has been described in detail elsewhere[16] and only its most important features will be described here. The spectrometer operates in the isochromat mode, which means that photons of a fixed energy ($\hbar\omega = 9.7$ eV) are collected, while the kinetic energy (E_k) of the electrons is swept in the range of 5 eV $< E_k < 25$ eV. The electrons traverse a field-free region before reaching the sample. The beam spot on the sample has a diameter of about 1 mm and the angular divergence is $\pm 5°$.

The electron gun is mounted coaxially with an ellipsoidal mirror, whose focal point coincides with the focal point of the electron gun. Light emitted from the sample into the entire 2π steradians of solid angle is (for all incident electron angles θ less than 35° from the normal) captured by the mirror and focused onto the detector. A Geiger-Müller tube of the type described by Denninger *et al.*[18] is used as photon detector. Its band pass is $\hbar\omega = 9.7 \pm 0.35$ eV. Count rates of several hundred counts per second are achieved with an incident electron current of about 1 μA. The sample chamber also contains a LEED system for sample characterization and orientation, facilities for retarding field Auger electron spectroscopy, a residual gas analyzer, and a noble-gas ion sputter gun.

Single-crystal Ta(100) samples were provided, oriented, cut, and mechanically polished by Oak Ridge National Laboratory. Following introduction into the vacuum chamber, the samples were cleaned solely by repeated flash anneals to a temperature of 3000 K for 15 sec. These high temperatures were necessary to remove surface oxygen, which was the final contaminant to be eliminated. After about 10 cycles, a crisp (1×1) low-energy electron diffraction (LEED) pattern was obtained. However, the inverse photoemission spectra were still rather featureless. After about 30 additional cycles, sharp well-defined

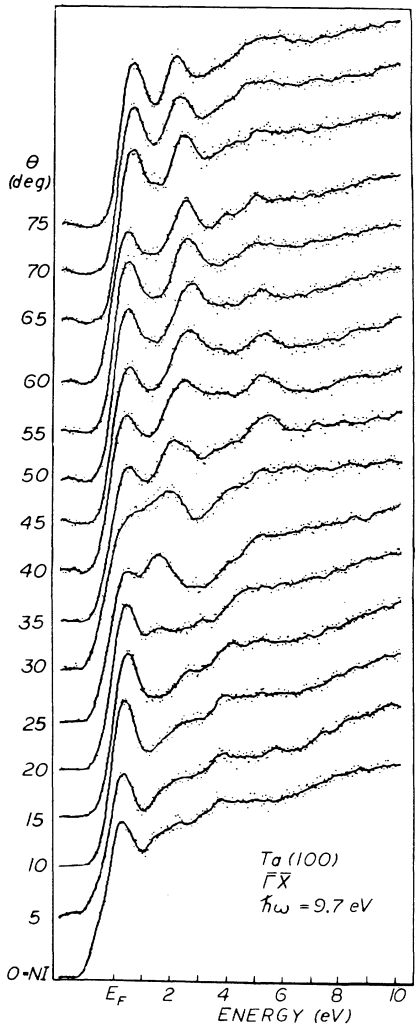

FIG. 2. Inverse photoemission spectra obtained from Ta(100) along the $\bar{\Gamma} \rightarrow \bar{X}$ azimuth at $\hbar\omega = 9.7$ eV.

features appeared, which were reproducible, unaffected by further cleaning, and quenched with small exposures to O_2 and H_2. At our base pressure of 2×10^{-10} Torr, the sharp features began to diminish after about 30 min. Consequently, data acquisition was limited to the first half-hour after a flash. Typically, the sample temperature was about 200°C at the start of data acquisition and the sample was flashed after each spectrum was obtained.

III. THE $\bar{\Gamma}\rightarrow\bar{X}$ AZIMUTH

Inverse photoemission spectra obtained from the $\bar{\Gamma}\rightarrow\bar{X}$ azimuth of the Ta(100) SBZ are shown in Fig. 2. At normal incidence, there is a single large feature at the Fermi energy (E_F) as well as several weaker features at higher energies. As the angle is increased, the emission about 0.5 eV is reduced and the feature near E_F is seen as a sharp peak. Near $\theta=25°$, this peak decreases in intensity, apparently dispersing below the Fermi level, and another peak near 1 eV gains intensity. The 1 eV peak then disperses away from the Fermi level, reaching a maximum energy of about 2.25 eV near $\theta=55°$. For larger angles, this new feature moves back toward E_F. Near $\theta=40°$, another peak appears close to E_F and moves to higher energies with larger angles.

The features which occur above 2 eV in this series of spectra show little sensitivity to surface contamination. Although sometimes weak, as in the $\theta=0°$ spectrum of Fig. 2, they are reproducible and occasionally quite well defined, as in the $\theta=35°$ spectrum. The sensitivity to surface contamination is demonstrated in Fig. 3, which shows a spectrum obtained as $\theta=45°$ for the clean surface before and after 5 L exposure to H_2. The features near the Fermi level and at 2 eV are strongly quenched by surface contamination, while the peak near 5 eV is only weakly affected. The 5 eV peak is therefore attributed to a bulk transition and the others to either surface states or surface resonances. Similar measurements at other angles indicate that the weak structure above about 1 eV near

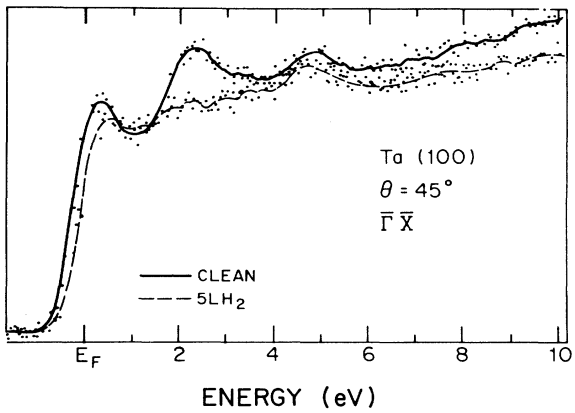

FIG. 3. Inverse photoemission spectra obtained at $\theta=45°$ along $\bar{\Gamma}\rightarrow\bar{X}$ from Ta(100). The solid spectrum is from the clean surface. The dashed spectrum was obtained after exposure of 5 L hydrogen.

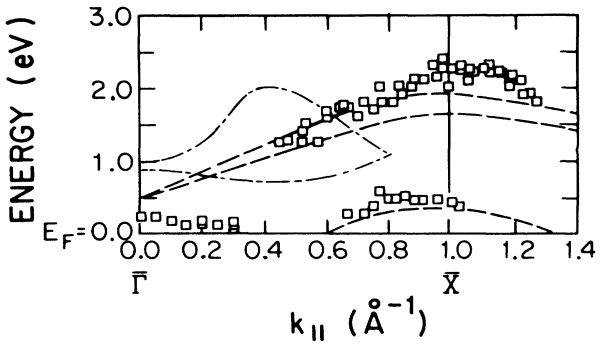

FIG. 4. Plot of energy versus $k_{||}$ of the surface-sensitive peaks from the spectra along $\bar{\Gamma}\rightarrow\bar{X}$. The dashed lines indicate calculated bulk bands while the solid short line around 0.5 $Å^{-1}$ is a calculated surface state (Ref. 10). The dot-dashed lines show the rigidly shifted band gap of W(100) from Ref. 20.

normal incidence and the features above about 2.5 eV in all spectra are bulk transitions and the rest are surface states and/or resonances. The bulk states will not be discussed further here.

Figure 4 shows the dispersion of the surface-sensitive features in the spectra in Fig. 2 as a function of $k_{||}$. In contrast to the surface states observed with inverse photoemission on many other surfaces,[15,16] the states seen here do not possess free-electron-like dispersions. Instead, the states disperse either not at all or have negative curvature, consistent with having significant d character. The curves in Fig. 4 are theoretically calculated band dispersions.[10] The solid parts of these curves correspond to states localized to the surface, while the dashed parts are bulklike. In the calculation,[10] surface states were (somewhat arbitrarily) defined as those that had more than 70% of their weight in the first layer. Since the surfaces of the slab are so close, the calculated bands occur in pairs, even and odd under z reflection. If the slab thickness were increased, these pairs would coalesce into a single band. Also shown (dash-dot curve) is the region corresponding to the projected absolute band gap of W(100) rigidly shifted 1.8 eV (Ref. 10).

The most striking feature of Fig. 4 is that the bands predicted to contain surface states correspond rather well to the dispersion of the experimentally observed surface-sensitive features. As the calculation predicts, a peak near E_F is only seen close to the SBZ center and then again near the SBZ boundary. Similar agreement is seen for the peak further away from E_F, which follows the predicted bands beyond the zone boundary into the second SBZ. Upon closer examination, however, it is clear the portions of the predicted dispersions expected to be bulklike correspond to experimental features that are extremely surface sensitive. According to the predictions, only a small region near E_F at $\bar{\Gamma}$ and another region around 1 eV above the Fermi level near 0.5 $Å^{-1}$ are expected to have states localized to the surface. The experimentally observed surface features exist over almost the entire SBZ, following the same bulk bands from which localized states are derived. It is possible that with a different criterion for dis-

tinguishing between surface and bulk states or the use of a thicker slab in the calculation, better agreement with experiments would be obtained.

The observation of a surface state above the Fermi level at $\bar{\Gamma}$ requires more discussion. Although a surface state is predicted by the calculation just above E_F in the vicinity of $\bar{\Gamma}$ (Ref. 10), this state is of even symmetry with respect to all mirror operations of the surface and expected to coalesce to a single state *below* the Fermi level in a calculation for a thicker film.[19] Angle-resolved photoelectron spectra[17,20] show a strong peak very close to the Fermi level at $\bar{\Gamma}$, identified as a surface state of totally even symmetry. If the prediction of a single surface state is correct, this observation, along with our inverse photoemission results described above, implies that the same surface state is observed both above and below the Fermi level. Such observations could be the result of either of two effects: finite experimental resolution or intrinsic broadening of the state.

Experimental artifacts can cause the effect if the dispersion of a surface state brings it above (below) E_F within the finite angular resolution of the instrument. In such a scenario, a feature could be seen in inverse photoemission (direct photoemission) even at angles where the state is actually below (above) the Fermi level. This is unlikely in our case since the experimental resolution in inverse photoemission is <0.2 Å^{-1} and in photoemission approximately equal to 0.1 Å^{-1}, yet the feature is observed experimentally for about 0.8 Å^{-1}.

A more likely explanation is that some broadening of this state occurs. Lifetime effects cannot be responsible, as they vanish for states at the Fermi level.[21] The state must therefore have a finite energy width, so that it spans the Fermi level before excitation. The probable origin of this width is coupling to bulk electronic states. As this does not occur for a true surface state in an absolute band gap, the state somehow overlaps the bulk bands. To investigate this possibility, we should examine the bulk bands of Ta projected onto the (100) surface.

As far as we know, no (100) projection of the Ta bulk bands has been published. However, the bulk bands of Ta are essentially rigidly shifted[10] with respect to those of W. We will therefore base the following discussion on a calculation of the projected bulk bands of W(100) (Ref. 22), with a shifted Fermi level, as an approximation for those of Ta. These bands are shown in Fig. 5 with the Ta Fermi level indicated. In the vicinity of the Fermi level, there is a continuum of states that are even with respect to reflections in the plane defined by the surface normal and the $\bar{\Gamma}\bar{X}$ line. However, there are no states near the Fermi level which are even in the $\bar{\Gamma}\bar{M}$ mirror plane, as illustrated by the large symmetry gap in Fig. 5(a). Coupling of an even surface state to the bulk bands is therefore symmetry forbidden along the $\bar{\Gamma}\bar{M}$ direction while this is not true along $\bar{\Gamma}\bar{X}$. Yet, as discussed above, the state is observed in both spectroscopies in the region approximately equal to 0.3 Å^{-1} away from $\bar{\Gamma}$ in the $\bar{\Gamma}\rightarrow\bar{M}$ direction. Therefore, this explanation as it stands cannot account for the origin of this width.

Up to this point, we have neglected the influence of relativistic effects. In the presence of spin-orbit interactions,

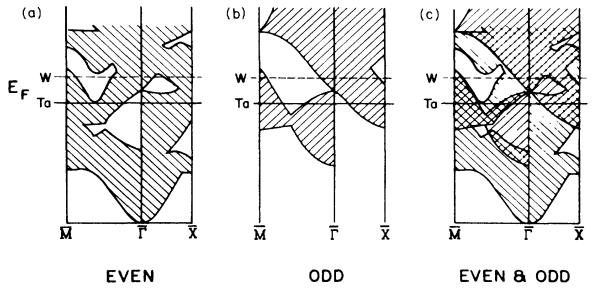

FIG. 5. The projected bulk electronic bands of W(100). The position of the Fermi level in Ta, assuming a rigid shift relative to W of 1.8 eV, is also shown. (a) shows the even bands, (b) shows the odd bands, and (c) shows the even and odd bands overlapped (after Ref. 22).

the even-odd classification used above is not rigorously valid.[9,23] This implies that the surface state may couple to bulk bands of either symmetry and will therefore be sharp only if it exists in an absolute gap. If we overlap the even [Fig. 5(a)] and odd bands [Fig. 5(b)], we find that there is no absolute gap near $\bar{\Gamma}$ [Fig. 5(c)]. The width of the surface states may then be due to weak coupling to bands of odd symmetry.

It is difficult to directly compare signal strengths in direct and inverse photoemission but, assuming a similar strength of the background signals, we conclude that the major part of the oscillator strength of this state is observed in *direct* photoemission and *not* in *inverse* photoemission. If the state would be entirely below the Fermi level without the broadening,[19] weak coupling would explain why the feature is stronger in the photoemission spectrum than in inverse photoemission.

It is interesting to compare this situation on Ta(100) with the one recently observed on Au(110).[16] There, a surface state in an *sp*-type band gap has been observed away from the surface normal in the $\bar{Y}$ gap. A relatively large feature is seen in inverse photoemission above the Fermi level, while in direct photoemission, on the other hand, a weak, quite asymmetric feature is seen below E_F. On Ta(100) the signal in direct photoemission appears to be the stronger one.

IV. THE $\bar{\Gamma}\rightarrow\bar{M}$ AZIMUTH

The results along the $\bar{\Gamma}\rightarrow\bar{M}$ azimuth are particularly important since the surface states on W(100) which occur in this direction have been related[10] to the reconstruction. Spectra taken from the $\bar{\Gamma}\rightarrow\bar{M}$ azimuth at various angles are plotted in Fig. 6. Again, a well-defined feature is observed near E_F at normal incidence. The intensity of the peak grows as it moves away from the Fermi level with increasing θ. Near $\theta=30°$, it broadens and appears to consist of two peaks, one at 0.5 eV and one at 1.0 eV. At $\theta=35°$ a single broad feature is seen at about 1 eV, subsequently developing a well-defined second peak at 1.5 eV. This new peak grows in intensity and disperses away from E_F as θ is increased, while the 1 eV peak disperses to lower energy. By $\theta=60°$, four features are seen in the

spectrum at about 0.5, 1.5, 2.5, and 4.5 eV. Figure 7 shows two spectra taken at this angle, one for a clean surface and another one after exposing to 1 L of oxygen. [1 langmuir (L) $\equiv 10^{-6}$ Torr sec.] All of the features below 4 eV are quenched, while the 4.5 eV feature, which we consequently relate to bulk emission, shows a much smaller effect.

We plot the dispersion of the surface-sensitive features of Fig. 6 with $k_{||}$ in Fig. 8, comparing again to the calculation by Krakauer.[10] The dot-dash line delineates the rigidly shifted even band gap from W(100) (Ref. 22). In this direction, aside from the feature near the Fermi level, most of the observed peaks occur in regions corresponding to the bulk band gap. The trends are fairly well reproduced by the predictions[10] but near the midpoint of the SBZ, significant discrepancies exist. The dispersion of the state around 2 eV agrees with a predicted band for part of the SBZ. The predicted surface state is expected to emerge already near $k_{||}=0.57$ Å^{-1}. In our inverse photoemission spectra, however, we do not see a feature until $k_{||}\approx 0.8$ Å^{-1} ($\theta=40°$, Fig. 6), well beyond the midpoint. For larger values of $k_{||}$, the observed state seems to follow

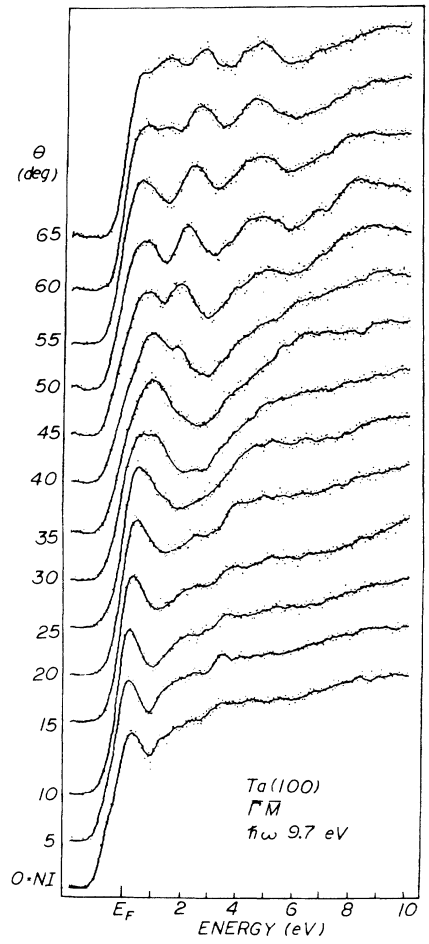

FIG. 6. Inverse photoemission spectra obtained from Ta(100) along the $\bar{\Gamma}\rightarrow\bar{M}$ azimuth at $\hbar\omega=9.7$ eV.

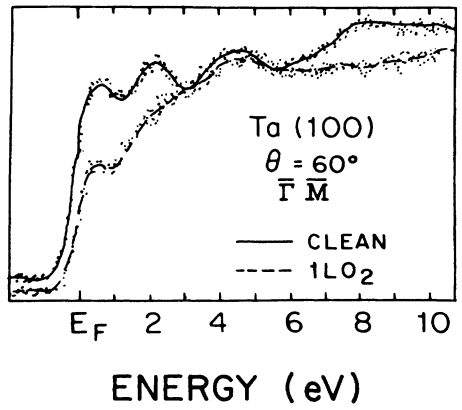

FIG. 7. Inverse photoemission spectra taken at $\theta=60°$ along $\bar{\Gamma}\rightarrow\bar{M}$. The solid curve is a clean spectrum and the dashed curve is obtained after exposure to 1 L of oxygen.

one branch of a z-reflected pair of states rather well. If the calculated dispersion for a thicker slab followed the average of the two bands, then the agreement would be satisfactory. If they favored the upper branch of this pair, then the disagreement would be on the level of that encountered for the surface states on W(100).[4]

The features which occur closer to the Fermi level at larger $k_{||}$ are not described as well by the calculation[10] over most of the SBZ (Fig. 8). The peak near the Fermi level at normal incidence does not disperse appreciably until about $k_{||}=0.4$ Å^{-1}. This is consistent with the angle-resolved photoemission measurements,[17] which show a peak near E_F up to about 0.4 Å^{-1}. As along the $\bar{\Gamma}\rightarrow\bar{X}$ azimuth, the features above and below the Fermi level are probably related. According to the calculation, this feature should at most exist for about 0.1 Å^{-1} near the center of the SBZ. For larger angles, the observed

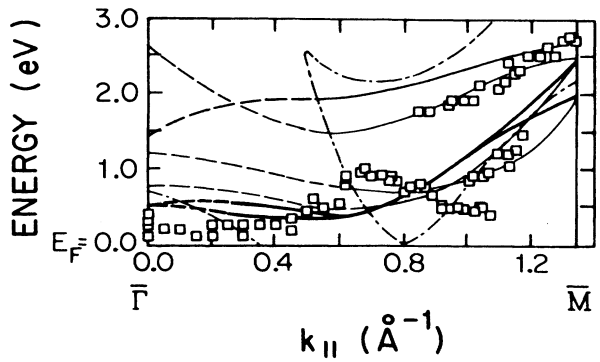

FIG. 8. The dispersion of the surface-sensitive features along $\bar{\Gamma}\rightarrow\bar{M}$ from the spectra in Fig. 6. The curves are the predicted dispersions of electronic bands from Ref. 10. The light (bold) bands are even (odd) in the plane. The solid parts are surface states and the dashed parts are bulk bands. The dot-dashed curve shows the rigidly shifted band gap of W(100) from Ref. 22.

peak (Fig. 8) disperses away from E_F. This behavior has no counterpart in the calculated surface states.

The observations described above refer mainly to quantitative discrepancies which may be eliminated with better experimental resolution and/or a more precise calculation. There are, however, several qualitative differences which deserve attention. The first instance occurs between 0.7 and 1.0 Å^{-1}, where the main peak in the spectra moves towards E_F. In this region, the predicted bands are either flat or disperse away from E_F. At $\theta=35°$, the peak is somewhat broad and less well defined, but it clearly does not follow the predicted[10] dispersion. The calculation shows that surface bands of both even and odd symmetry are expected in this region. It would be useful to vary the photon detection angle in the experiment to determine the symmetry of the states experimentally. Unfortunately, our apparatus does not provide this capability.

The second qualitative difference is seen for $k_{\|} > 1.0$ Å^{-1}. The dispersion of the weak feature near 1 eV agrees well with the calculated bands, however, an additional peak of unclear origin appears near the Fermi level. There is no pronounced feature near the Fermi level in the corresponding angle-resolved photoelectron spectra,[17] indicating that this peak probably does not disperse into the occupied bands. As Fig. 7 illustrated, this feature is sensitive to contamination, indicating that it is a surface state or surface resonance, which does not appear in the calculation.

The intensity, as compared to the background, of the *d*-like surface states discussed above does not appear to be significantly different from that of the *sp*-derived surface states on Au(110) (Ref. 16). The *sp*-like states of Cu(110) (Ref. 16) are, on the other hand, more intense than those seen on either Au(110) or Ta(100). In general, all of the primary features, as normalized to the inelastic background, in our inverse photoemission spectra, be they bulk or surface related, are weaker for the $5d$ metals than for the $3d$ metals. It is possible that this difference is due to changes in the background intensity and not an overall change in the primary signal. The similarity of the angle-integrated spectra obtained by Boiziau *et al.*[13] at $\hbar\omega=9.7$ eV with their core-level appearance-potential-spectroscopy data have been interpreted by them to indicate that matrix element effects are not of primary importance for Ta. They have also pointed out the importance of electron-hole pair contributions to the shape of the spectra. The background is produced mainly by primary electrons which suffer energy losses by electron-hole pair creation and then decay by a photon-mediated transition.[24] The k vector of the transition is therefore ill defined and the background will reflect the density of states above the Fermi level. As one moves down the Periodic Table from Cu (Refs. 25 and 26) to Au (Ref. 27) the density of states for the first 10 eV above the Fermi level increases by about a factor of 2. This doubling is repeated again upon going from Au to Ta (Refs. 27 and 14) as Ta has a large band of unoccupied $5d$ states. This can account, at least in part, for the relative weakness of the primary features.

Since the bulk bands of Ta are essentially rigidly shifted from the bulk bands of W, it is interesting to investigate

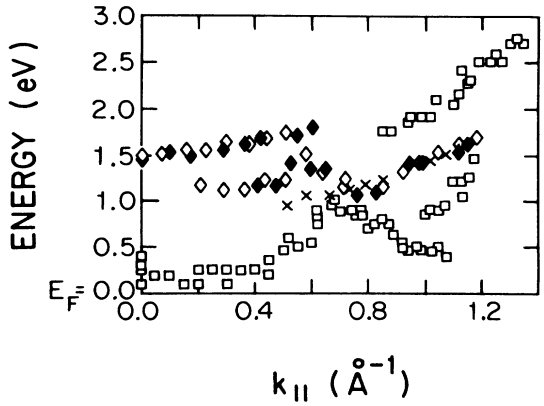

FIG. 9. Comparison of direct photoemission data (from Ref. 4) for W(100), rigidly shifted 1.8 eV, and the Ta(100) inverse photoemission data (open squares, from Fig. 8) as a function of parallel wave vector in the $\bar{\Gamma}\rightarrow\bar{M}$ azimuth. The crosses denote states with (mainly) odd symmetry, while the diamonds are states of (mainly) even symmetry (open symbols $\hbar\omega=22$ eV, solid symbols $\hbar\omega=18$ eV). $\bar{M}$ for W is located at 1.4 Å^{-1} and for Ta at 1.35 Å^{-1}.

the extent to which the surface states on Ta(100) can be understood on the basis of a rigid shift of the states on W(100). High-resolution direct photoemission data for W(100) exist for the $\bar{\Gamma}\rightarrow\bar{M}$ azimuth,[4] and in Fig. 9 we plot these data, rigidly shifted 1.8 eV, as well as the inverse photoemission data from Fig. 8. In the region of interest, direct photoemission from W(100) shows three surface states: The well-known "Swanson hump" (SH),[4,5] of even symmetry, with a binding energy at $\bar{\Gamma}$ of 0.3 eV relative to E_F, and a doublet (D) surface state, with both an even and an odd component, crossing the Fermi level at 1.2 Å^{-1}.[4,5]

Krakauer's calculation associates the surface state at E_F on Ta with the SH state of W(100). Our experimental observations at $\bar{\Gamma}$ are consistent with this interpretation. As was the case for W(100), however, the measured dispersions of these features differ significantly from the predictions. We see from Fig. 9 that, in general, the relationship between surface states on W(100) and on Ta(100) is more complicated than that implied by a simple rigid-band model. There are states on Ta(100) for which there are no counterparts on W(100) and the dispersions of the other states are significantly different from one metal to the other. The overlap of even and odd surface state dispersions suggests that it would be useful to study the polarization dependence of the emission. We note also that there is a counterpart in the W data to the irregularity in the dispersion of the Ta states around 0.65 Å^{-1}. In neither the tungsten case nor the tantalum one, is there anything corresponding to this in the calculated dispersions.

V. SUMMARY

Essentially all of the well-defined features within 2 eV of the Fermi level in the inverse photoemission spectra

from Ta(100) show strong sensitivity to surface contamination and we have therefore associated them with surface states and/or resonances. The features above 2 eV tend to be weak, with the exception of peaks occurring near the $\bar{X}$ and $\bar{M}$ points on the SBZ boundary, and are relatively insensitive to surface contamination. The dispersion of the surface states and/or resonances are in semiquantitative agreement with predictions by Krakauer.[10] A detailed comparison shows, however, that the observed features often exist in different regions of the SBZ than expected from the calculation. The discrepancies between the observed dispersions and those predicted are on the same order as the splitting between even and odd z-reflected surface state pairs in the calculation. It is therefore difficult to say whether the level of agreement here is better than was obtained earlier between photoemission measurements from W(100) (Ref. 4) and a slab calculation for that surface.[8] In this sense, our results do not strongly support the view that the surface states on W(100) play an important role in the reconstruction of that surface.

The surface-sensitive spectral features exhibit dispersions which cannot be fit with free-electron-like parabolas. Instead, the dispersions are rather flat and sometimes concave downward as expected for d-derived states. The intensity of these d-like surface states is not significantly different from that of sp-derived states above the Fermi level in Au (Ref. 16). When compared to the background, however, they are significantly weaker than similar sp states on Cu (Ref. 16) and Ag (Ref. 15). This may be because of the higher density of unoccupied states immediately above the Fermi level for the $5d$ metals as compared to the $3d$ metals. A peak seen at the Fermi level for the normal incidence spectrum seems to be related to a strong surface state or resonance below the Fermi level broadened in the ground state so that it spans the Fermi level. This broadening may be due to coupling with the bulk bands.

Note added: Very recently, F. Himpsel *et al.* (private communication) have observed d-derived unoccupied surface states on W(100) and Mo(100) close to the Fermi level, similar to the case of Ta(100).

ACKNOWLEDGMENTS

We thank Dr. D. M. Zehner for generously supplying the crystals, and Dr. R. A. DiDio, Dr. Zehner, and Dr. E. W. Plummer for discussions. This research was supported by the National Science Foundation (Materials Research Laboratory Program) under Grant No. DMR-85-19059.

*Present address: Department of Physics and Astronomy, Rutgers University, P.O. Box 849, Piscataway, NJ 08854.

[1]T. E. Felter, R. A. Barker, and P. J. Estrup, Phys. Rev. Lett. **38**, 1138 (1977).
[2]M. K. Debe and D. A. King, Phys. Rev. Lett. **39**, 708 (1977).
[3]M. K. Debe and D. A. King, J. Phys. C **10**, L303 (1977).
[4]M. I. Holmes and T. Gustafsson, Phys. Rev. Lett. **47**, 443 (1981).
[5]S. L. Weng, E. W. Plummer, and T. Gustafsson, Phys. Rev. B **18**, 1718 (1978).
[6]E. Tossatti, Solid State Commun. **25**, 637 (1978).
[7]J. E. Inglesfield, J. Phys. C **12**, 149 (1979).
[8]H. Krakauer, M. Posternak, and A. J. Freeman, Phys. Rev. Lett. **43**, 1885 (1979).
[9]L. F. Mattheiss and D. R. Hamann, Phys. Rev. B **29**, 5372 (1984).
[10]H. Krakauer, Phys. Rev. B **30**, 6834 (1984).
[11]A. Titov and W. Moritz, Surf. Sci. **123**, L709 (1982).
[12]S. T. Ceyer, A. J. Melmed, J. J. Carroll, and W. R. Graham, Surf. Sci. **144**, L444 (1984).
[13]C. Boiziau, V. Dose, and H. Scheidt, Phys. Status Solidi B **93**, 197 (1979).
[14]L. F. Mattheis, Phys. Rev. B **1**, 373 (1970); J. Petroff and C. R. Viswanathan, *ibid.* **4**, 799 (1971).
[15]B. Reihl, R. R. Schlitter, and H. Neff, Phys. Rev. Lett. **52**, 1826 (1984).
[16]R. A. Bartynski and T. Gustafsson, Phys. Rev. B **33**, 6588 (1986).
[17]R. A. DiDio, D. M. Zehner, S. C. Lui, and E. W. Plummer (unpublished).
[18]G. Denninger, V. Dose, and H. Scheidt, Appl. Phys. **81**, 375 (1979).
[19]H. Krakauer (private communication).
[20]P. Soukiassian, R. Riwan, J. Lecante, E. Wimmer, S. R. Chubb, and A. J. Freeman, Phys. Rev. B **31**, 4911 (1985).
[21]See, for example, L. Hedin and S. Lundqvist, in Solid State Physics, edited by F. Seitz, P. Turnbull, and H. Ehrenreich (Holt, Reinhardt and Winston, New York, 1969), Vol. 23, p. 1.
[22]W. R. Grise, D. G. Dempsey, L. Kleinman, and K. Mednick, Phys. Rev. B **20**, 3045 (1979).
[23]J. Callaway, *Energy Band Theory* (Academic, New York, 1964) pp. 46–51.
[24]V. Dose, Prog. Surf. Sci. **13**, 225 (1983).
[25]J. F. Janak, A. R. Williams, and V. L. Moruzzi, Phys. Rev. B **11**, 1522 (1975).
[26]G. A. Burdick, Phys. Rev. **129**, 138 (1963).
[27]N. E. Christensen and B. O. Seraphin, Phys. Rev. B **4**, 3321 (1971).